Intact Protein Detection

DOI: 10.1002/anie.200((will be filled in by the editorial staff))

Enhanced Detection of High Mass Proteins Using an Active Pixel Detector**

Shane R. Ellis, Julia H. Jungmann, Donald F. Smith, Jens Soltwisch and Ron M. A. Heeren

Since their emergence in the 1980s, matrix-assisted laser desorption/ionization (MALDI)[1] and electrospray ionization (ESI)[2] have widely been applied to analysis of proteins and have been key drivers in the growth of the proteomics field.[3] A significant difference between the two ionization techniques is that MALDI, unlike ESI, typically produces singly or doubly charged ions for large molecules and therefore requires mass analysers and ion detection approaches suitable for these higher *m/z* species. MALDI is often coupled with time-of-flight (TOF) mass analysers due to their theoretically unlimited mass range. However, in practice such systems are ultimately limited by the ability to efficiently detect singly charged high *m/z* ions. Ion detection in TOF-mass spectrometry (TOF-MS) is traditionally accomplished using the ion-to-electron conversion abilities of microchannel plates (MCPs). However, the ion-to-electron conversion efficiency of an MCP is well known to decrease with decreasing ion velocity (*i.e.*, at higher mass).[4] Thus, although many high mass ions can be generated, they may not be efficiently detected and their observed ion abundance may appear artificially low or possibly not be detected at all. To overcome this, a variety of alternative non-MCP-based ion detection systems have been developed and have been demonstrated for *m/z* values up to 1MDa. [4b, 5] In this paper we describe the first implementation of the Timepix active pixel detector[6] on a commercial MALDI linear-TOF instrument that provides ion acceleration voltages up to 25 kV. This combination of high ion acceleration voltages and a highly sensitive pixelated detector are shown to allow detection of high *m/z* ions up 400 kDa using MCP-based detection with significant enhancements in signal-to-noise compared with conventional detection approaches. The results presented demonstrate the advantages offered by a highly parallelized detection system in TOF-MS.

The detector assembly used in this study is identical to that previously described.[7] The detector consists of a 512 × 512 detector array and thus provides 262144 parallel detectors where each pixel is a single-stop time-to-digital converter (TDC). The Timepix is operated in time-of-flight mode where the arrival time with respect to an external trigger is measured. Further details are provided in reference [6a] and the Supporting Information. For all experiments both Timepix and MCP/analog-to-digital converter (ADC) spectra were acquired simultaneously from the same laser shots. The latter was achieved by recording the current pulse from the high voltage line of the MCP backside and then digitizing this analog signal with the standard ADC system of the TOF mass spectrometer[6a]

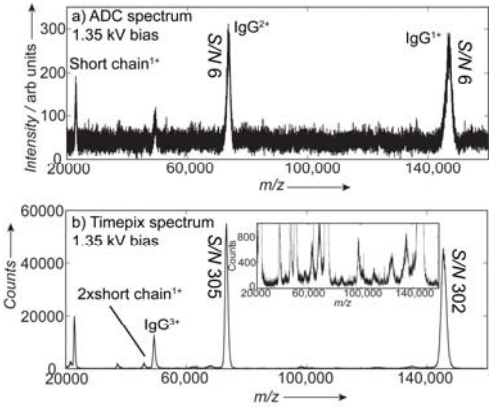

Figure 1. (a) MALDI-TOF spectrum of Immunoglobulin G (IgG) acquired using the decoupled MCP signal in combination with an analog-to-digital converter following baseline correction. (b) Corresponding IgG spectrum acquired with the Timepix system without any post- processing. Both spectra were acquired in parallel with an MCP bias of 1.35 kV and the accumulation of 500 laser shots. The inset of (b) shows the enlarged low counts region of (b) revealing the low abundance ions. Signal-to-noise (S/N) values are indicated.

Analysis of a standard protein mix spanning ~*m/z* 22000-66500 with the Timepix generated spectra with up to a ~30-fold improvement in signal-to-noise compared to the corresponding ADC spectrum acquired with an identical (1.35 kV) MCP bias. (Figure S1). The high mass detection capabilities of the Timepix detector were further evaluated by the analysis of the antibody Immunoglobulin G (IgG, MW ~150 kDa). Figure 1a shows the MALDI-MS spectrum of IgG acquired from the decoupled MCP signal using an MCP bias of 1.35 kV and the accumulation of 500 laser shots with baseline correction. The single and doubly charged IgG ions are observed at *m/z* values of 147,000and 73,000, respectively, in addition to an ion observed at *m/z* 23,000 that may be assigned to a single short chain fragment of IgG.[8] Figure 1b shows the corresponding Timepix spectrum acquired in parallel with the MCP spectrum (Figure 1a). The Timepix spectrum reveals a series of IgG related ions with over an order of magnitude increase in signal-to-noise. In addition to the singly and doubly charged IgG and the short chain fragment observed in the MCP spectrum, the enhanced signal-to-noise of the Timepix also allows detection of several other IgG-related ions. For example the ion at *m/z* 49,000 can be assigned to either triple charged IgG or a single heavy fragment (or a combination thereof) while the ion at *m/z* 46,000

[*] Dr. Shane R. Ellis, Dr. Julia H. Jungmann, Dr. Don F. Smith, Dr. Jens. Soltwisch and Prof. Dr. Ron M. A. Heeren
Biomolecular Imaging Mass Spectroemtry
FOM Institute AMOLF
Science Park 104, 1098 XG Amsterdam, The Netherlands
Fax: +31-20-7547290
E-mail: heeren@amolf.nl

[**] * Part of this research is supported by the Dutch Technology Foundation STW, which is the Applied Science Division of NWO, and the Technology Programme of the Ministry of Economic Affairs, Project OTP 11956. This work is part of the research program of the Stichting voor Fundamenteel Onderzoek der Materie (FOM), which is financially supported by the Nederlandse organisatie voor Wetenschappelijk Onderzoek (NWO). The authors are grateful to Ronald Buijs for electronics support and Gert Eijkel for development of data analysis software.

Supporting information for this article is available on the WWW under http://www.angewandte.org

maybe assigned to a fragment consisting of the two short chains. The inset shows an enlarged region of the low abundance IgG-related ions detected with the Timepix. This spectrum reveals a sequence of low abundance ions that are not observed in the ADC spectrum. Enhanced spectra are also obtained for high *m/z* ions when operating at higher (1.70 kV) MCP gains, although as expected at higher MCP gains the relative performance of the ADC system is improved. This also highlights the greater charge sensitivity of the Timepix. (Supporting Information Figure S2 and Figure S3).

The enhanced detection offered by the Timepix compared to the ADC system is the result of several factors. First, the threshold charge required for a single Timepix TDC to record an event is set at a level above the intrinsic electronic noise of the Timepix application specific-integrated circuit (ASIC). As a result, every recorded 'hit' is the result of an actual ion arrival event at the detector, and thus constitutes a real signal that contributes to the intensity of the particular *m/z* value. For a pixel to record an event, approximately 600 electrons (or other charges) need to be deposited into a pixel within 50 ns. Importantly, this charge density is easily produced by a dual MCP stack. Secondly, the footprint of the electron shower produced by the MCPs from a single ion event impinging on the detector spans ~30-100 pixels, *i.e.,* the detection of a single ion is effectively oversampled by a factor of ~30-100 (See Supporting Information Figure S4). Furthermore, the 512x512 pixel array is capable of recording the simultaneous arrival of ions of multiple ions as separate events, so long as they strike different areas of the detector. This provides a highly paralleled and multiplexed detection system with a high dynamic range, in particular if the ions arrived spatially distributed.[6a] By contrast, detection with an ADC integrates the current pulses produced by the MCP upon impact of simultaneously arriving ions. While this approach is also capable of detecting simultaneously arriving ions by virtue of the greater MCP current produced by multiple ions with the same TOF, it still provides lower signal-to-noise than the Timepix at these MCP gains (Figure 1). The digitization of measurement frames by the ADC is also susceptible to electronic noise. To minimise the interference of this electronic noise, ADC systems incorporate a low level threshold trigger such that low magnitude pulses are discriminated. As a result, when operating at sub-saturation MCP gains (*i,e.,* 1.35 kV), the pulse height of many ion events is not sufficient to exceed this ADC threshold and the event is not registered above the noise. By contrast, the paralleled detection of the Timepix can readily detect individual ions arriving from a single laser pulse with high signal-to-noise (Supporting Information Figure S5).

To evaluate the Timepix for detection of proteins >150 kDa, detection of the antibody Immunoglobulin A (IgA, MW ~400 kDa) was also investigated. Figure 2a shows the ADC spectrum acquired from 5000 accumulated laser shots with an MCP bias of 1.70 kV. The doubly charged ion of intact IgA can be observed at *m/z* 200,000, while the single charged ion at *m/z* 400,000 is also observed, albeit with low signal-to-noise. A series abundant lower mass ions were also observed and likely indicate dissociation of intact IgA during the desorption/ionization process (data not shown). The corresponding Timepix spectrum acquired with the same MCP gain is shown in Figure 2b. Similar to the spectra shown above, the Timepix provides a significant improvement in signal-to-noise compared to the ADC spectrum acquired at the same gain. Crucially, the singly charged IgA ion at ~*m/z* 400,000 is easily observed. Note that this Timepix spectrum consists of two stitched spectra. The first spectrum was acquired with an acquisition window beginning 415 µs after the laser shot such that double charged IgA is one of the first arriving ions. The second window was acquired with a delay of 600 µs such that single charged IgA is one of the first arriving ions. This analysis enhances the detection of higher *m/z* which may otherwise be discriminated against due to the single stop nature of the Timepix TDCs and the large footprint of singe-ion induced electron showers at higher MCP gains. While detection of both doubly and singly charged IgA in the same window provides less signal intensity for the singly charged ion, the signal-to-noise is still greater than that observed in the ADC spectrum (see Supporting Information Figure S6). Given the decrease in efficiency of the ion-to-electron conversion of MCPs with decreasing ion momentum (*i.e.,* at higher *m/z*),[4a, 4c] the ability to detect intact protein ions at ~*m/z* 400,000 with an MCP-based detection system is remarkable and corresponds to a four-fold increase in mass range than previous Timepix studies[6a, 9]. Although polymers approaching 1 MDa have been detected with an MCP under certain conditions,[10] the increased detection efficiency of individual MCP electron showers offered by the Timepix provides a means to extend the dynamic range[6a] as well as the accessible mass range of MCP-based detection systems in TOF-MS.

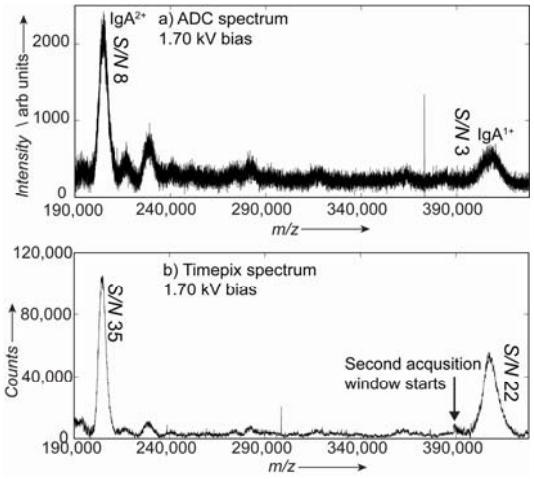

Figure 2. (a) MALDI-TOF spectrum of Immunoglobulin A (IgA) acquired using the decoupled MCP signal in combination with an analog-to-digital converter. (b) Corresponding IgG spectrum acquired with the Timepix system. The Timepix spectrum has been generated by stitching together two acquisition windows such that the second window begins just before the arrival of single charged IgA (indicated by arrow). The corresponding Timepix spectrum acquired from a single acquisition window is provided as Supporting Information (Figure S6) Both spectra were baseline corrected and were acquired with an MCP bias of 1.70 kV and are the sum of 5000 laser shots. Signal-to-noise (S/N) values are indicated.

An important advantage of the Timepix detector compared to conventional detection systems is its ability to simultaneously acquire both the arrival time and position of incoming ions. While the former is a necessity for mass spectrometric analysis, the ability to directly visualise the spatial distribution of incoming ions with a specific *m/z* can help provide insights into the fundamental processes and their dynamics that occur during ion formation and extraction through the ion source region. Additionally, this provides the researcher with the capability to quickly optimise extraction and

focussing parameters to increase ion signal for the mass range of interest by visualising in real time the ion density reaching the detector. Figure 3 shows an overlay of the integrated images from 500 laser shots for 3 different ions acquired during acquisition of the Timepix spectra shown in Figure 1b and Figure S1b. These images show the spatial distribution of arriving ions within the ion cloud colour-coded for their different TOFs in the detector plane and reveal mass-dependant ion focussing phenomena. Figure 3a shows the integrated images of Protein A^{2+} (*m/z* 22307), Protein A^{1+} (*m/z* 44613) and BSA^{1+} (*m/z* 66500) acquired with an extraction voltage of 1.9 kV and the Einzel lens set to 6 kV. Protein A^{2+} (shown in red) is clearly seen to be space-focussed onto the detector, although some distortion of the ion cloud is seen through the observation of a cross-like shape. By contrast the higher *m/z* Protein A^{1+} ion (shown in green) is focussed to a slightly larger area of the detector that is partly offset from that observed for the double charged ion. The heavier singly charged BSA ions (shown in blue) are not as tightly focussed on the detector, and interestingly, are observed in a cross-like shape offset from that of Protein A^{2+} by an angle of 45 degrees. A different situation is observed for the analysis of IgG with an extraction voltage of 4 kV and the Einzel lens set to 12 kV (Figure 3b). The short chain fragment (*m/z* 23,000, shown in red), double charged IgG (*m/z* 74000, shown in green) and single charged IgG (*m/z* 147,000, shown in blue) are all observed to observed to have circular distributions with the diameter increasing with increasing *m/z*. A similar distribution is also observed for analysis of the protein mix (*m/z* 22,000-66,500) when acquired with the same ion extraction parameters (data not shown). These data indicate fascinating mass-dependent ion focussing effects that may also be dependent on the initial plume dynamics prior to extraction and the origin of these effects are currently under investigation. The observation of such mass-dependant focussing phenomena is also advantageous for acquisition of Timepix spectra across a wide mass range. As each pixel is only capable of recording a single event for each acquisition cycle (laser shot), if all ions were focused to the same area of the detector, later arriving ions would not detected efficiently as the available pixels within the focused area would have already been utilised for detection of lighter, earlier arriving ions. However, the fact that ions of different masses are observed to strike different regions of the detector helps minimise suppression due to the single hit capacity of the Timepix, particularly at the high count rates typically encountered during MALDI.

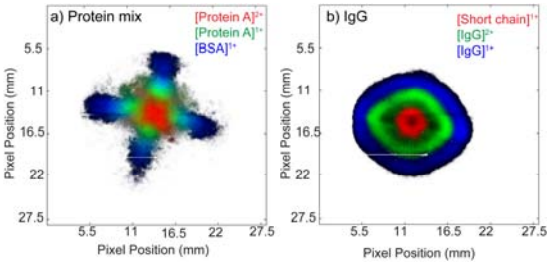

Figure 3. Imaging of ion cloud distributions as projected onto the detector. (a) Ion cloud distributions of Protein A^{2+} (*m/z* 22307, shown in red), Protein A^{1+} (*m/z* 44613 shown in green), and Bovine serum albumin (BSA) (*m/z* 66500 shown in blue) when acquired with an extraction voltage of 1.9 kV, lens voltage of 6 kV and pulsed ion extraction (PIE delay) of 500 ns. (b) Ion cloud distributions of Immunoglobulin G (IgG) short chain fragment (*m/z* 23000, shown in red), IgG^{2+} (*m/z* 73000, shown in green), and IgG^{1+} (*m/z* 147000, shown in blue) when acquired with an extraction voltage of 4 kV, lens voltage of 12 kV and pulsed ion extraction (PIE) delay of 500 ns. Both images represent the accumulation of 500 laser shots and were acquired with an MCP bias of 1.35 kV.

This paper describes the implementation of the Timepix detection system on a commercial linear time-of-flight mass spectrometer. This coupling allows the high (25 kV) ion acceleration voltages typically available on such instruments to be exploited for detection of high mass ions with greater efficiency compared with conventional ADC and TDC detection technologies. While Timepix detection is still ultimately limited by the decreased ion-to-electron conversion of slower (higher *m/z*) ions, by allowing more efficient collection of MCP electron showers it provides a method to extend the accessible mass range of MCPs. Moreover, the ability to acquire high quality spectra at lower MCP gains is also offers advantageous in terms increased MCP lifetime, reduced dead time due to MCP charge depletion and for exploiting the imaging capabilities of the Timepix. These direct imaging capabilities allow visualisation of mass-dependent ion focussing effects occurring during ion extraction that can provide insight into both ion optical processes and possibly the dynamics of the MALDI plume itself. These results demonstrate the enhanced detection capabilities offered by massively parallel detection with charge-sensitive pixel detectors in TOF-MS.

Experimental Section

All protein samples were mixed with sinapinic acid (20 $mg.mL^{-1}$ in acetonitrile:water (v:v) + 0.1% TFA). 1 µL aliquots of each analyte:matrix solution were then deposited onto a stainless steel target plate and air dried prior to analysis. All mass spectrometry experiments were performed on an Ultraflex III MALDI TOF-MS (Bruker Daltonik GmbH, Bremen, Germany) equipped with a Smartbeam 355 nm Nd:YAG laser and with an acceleration voltage of 25 kV. Further details regarding sample preparation, MS acquisition, the detector assembly and data acquisition are provided as Supporting Information.

Received: ((will be filled in by the editorial staff))
Published online on ((will be filled in by the editorial staff))

Keywords: proteins, mass spectrometry MALDI, high mass detector

[1] a) M. Karas, D. Bachmann, U. Bahr, F. Hillenkamp, *Int J Mass Spectrom Ion Process.* **1987**, *78*, 53; b) K. Tanaka, H. Waki, Y. Ido, S. Akita, Y. Yoshida, T. Yoshida, T. Matsuo, *Rapid Commun. Mass Spectrom.* **1988**, *2*, 151.

[2] J. B. Fenn, M. Mann, C. K. Meng, S. F. Wong, C. M. Whitehouse, *Science* **1989**, *246*, 64.

[3] a) R. Aebersold, M. Mann, *Nature* **2003**, *422*, 198; b) X. Han, A. Aslanian, J. R. Yates Iii, *Curr. Opin. Chem. Biol.* **2008**, *12*, 483; c) J. Godovac-Zimmermann, L. R. Brown, *Mass Spectrom. Rev.* **2001**, *20*, 1; d) K. E. Burnum, S. L. Frappier, R. M. Caprioli, *Annu. Rev. Anal. Chem.* **2008**, *1*, 689; e) M. Stoeckli, T. G. Schhaaf, P. Chaurand, R. M. Caprioli, *Nat. Med.* **2001**, *7*, 493.

[4] a) X. Chen, M. S. Westphall, L. M. Smith, *Anal. Chem.* **2003**, *75*, 5944; b) B. Spengler, D. Kirsch, R. Kaufmann, M. Karas, F. Hillenkamp, U. Giessmann, *Rapid Commun.*

Mass Spectrom. **1990**, *4*, 301; c) G. Westmacott, M. Frank, S. E. Labov, W. H. Benner, *Rapid Commun. Mass Spectrom.* **2000**, *14*, 1854.

[5] a) M. A. Park, J. H. Callahan, A. Vertes, *Rapid Commun. Mass Spectrom.* **1994**, *8*, 317; b) D. C. Imrie, J. M. Pentney, J. S. Cottrell, *Rapid Commun. Mass Spectrom.* **1995**, *9*, 1293; c) A. Remoortere, R. van Zeijl, N. van den Oever, J. Franck, R. Longuespée, M. Wisztorski, M. Salzet, A. Deelder, I. Fournier, L. McDonnell, *J. Am. Soc. Mass Spectrom.* **2010**, *21*, 1922; d) O. Yanes, F. X. Avilés, R. Wenzel, A. Nazabal, R. Zenobi, J. J. Calvete, *J. Am. Soc. Mass Spectrom.* **2007**, *18*, 600; e) R. J. Wenzel, U. Matter, L. Schultheis, R. Zenobi, *Anal. Chem.* **2005**, *77*, 4329.

[6] a) J. H. Jungmann, L. MacAleese, J. Visser, M. J. J. Vrakking, R. M. A. Heeren, *Anal. Chem.* **2011**, *83*, 7888; b) X. Llopart, R. Ballabriga, M. Campbell, L. Tlustos, W. Wong, *Nucl. Instrum. Methods. Phys. Res. A.* **2007**, *581*, 485.

[7] A. Kiss, J. H. Jungmann, D. F. Smith, R. M. A. Heeren, *Rev. Sci. Instrum.* **2013**, *84*, 013704.

[8] H. Liu, G. Gaza-Bulseco, C. Chumsae, A. Newby-Kew, *Biotechnol. Lett.* **2007**, *29*, 1611.

[9] J. H. Jungmann, D. F. Smith, A. Kiss, L. MacAleese, R. Buijs, R. M. A. Heeren, *Int. J. Mass Spectrom.* **2013**, *341-342*, 34.

[10] D. C. Schriemer, L. Li, *Anal. Chem.* **1996**, *68*, 2721.

Entry for the Table of Contents (Please choose one layout)

Layout 1:

((Catch Phrase))

Shane R. Ellis, Julia H. Jungmann, Donald F. Smith Jens Solwisch and Ro M. A Heeren

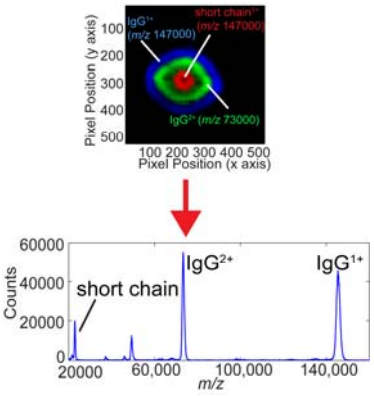

Enhanced Detection of High Mass Proteins Using an Active Pixel Detector

Implementation of an active pixel detector with high charge sensitivity on a linear time-of-flight mass spectrometer is shown to provide:

i) Enhanced detection of high mass proteins with a conventional microchannel plate detector and thereby provides a means to extend the mass range of such detectors.

ii) Direct visualisation of mass-dependent ion focussing phenomena occurring during ion extraction.

Layout 2:

((Catch Phrase))

((Author(s), Corresponding Author(s)*))
_____ Page – Page

((TOC Graphic))

((Title Text))

((Text for Table of Contents, max. 450 characters))

Angewandte Chemie
Eine Zeitschrift der Gesellschaft Deutscher Chemiker

Supporting Information

69451 Weinheim, Germany

Enhanced Detection of High-Mass Proteins by Using an Active Pixel Detector**

*Shane R. Ellis, Julia H. Jungmann, Donald F. Smith, Jens Soltwisch, and Ron M. A. Heeren**

anie_201305501_sm_miscellaneous_information.pdf

Experimental Methods

The Timepix Active Pixel Detector

The Medipix/Timepix detectors have been developed within the CERN hosted Medipix collaboration (www.cern.ch/medipix). Originally designed for high energy physics applications, the Medipix2[1] and Timepix[2] chips have dimensions of 1.4 × 1.6 cm^2 and consist of an array of 256 × 256 individual pixels with a pitch of 55 μm^2. In this study a 2 × 2 chip array is used, providing a 512 × 512 pixel array for detection. For high energy physics applications (such as X-ray and electron detection), the chips are often used in combination with a thin semiconductor sensor layer bump bonded to each pixel. For ion detection such as that required in this study, microchannel plates (MCPs) are used as an intermediate ion-to-electron conversion medium in combination with bare chips (without the sensor layer). For more detail refer to reference.[3]

Each Timepix pixel is capable of operating in one of three modes: (1) event counting mode where each pixel simply counts the number of arriving particles; (2) Time over threshold mode where the time the generated charge from an arriving particle allows a pixel to stay over the detection threshold is measured and; (3) Time-of-flight mode where the arrival time with respect to an external trigger is measured. In this study time-of-flight mode is exclusively used and the Timepix clock is operated at 40 MHz (25 ns time bins). The clock rate, in combination with the counter depth of 11810, provides a maximum measurement window of 295 μs. Importantly, each pixel is a single-stop time-to-converter (TDC) meaning each pixel can only record a single event per measurement frame.

The detector assembly used in this study is identical to that previously described.[4] Briefly the 2 × 2 Timepix chip array was mounted 2 cm behind a chevron MCP stack having an active area of 4 cm, 12 μm pores and 15 μm pitch. Homemade power supplies were used

to supply the MCP high voltages. The back MCP was held at 400 V while for Timepix spectral acquisition the potential on the front MCP was typically 1.75-2.1 kV (providing a bias across the MCPs 1.35-1.70 kV). The Timepix chips are held at ground potential. The trigger for the Timepix acquisition window was supplied by a pulse and delay generator (DG535, Stanford Research Systems, CA, USA) with the matrix-assisted laser desorption ionization (MALDI) laser trigger used as the input signal. Chip control and data acquisition is handled with the dedicated "Pixelman" software.[5] Timepix data is readout via a dedicated 1 $Gbit.s^{-1}$ Ethernet read-out system.[6] All data analysis and mass calibration was performed using in house developed software written in MATLAB (Matlab; Mathworks, Natick, MA, USA; ver. 7.13.0.564, R2010b).

Materials

All solvents, sinapinic acid, Immunoglobulin G (IgG, from goat serum) and Immunoglobulin A (IgA, from human colostrums) were purchased from Sigma-Aldrich (Zwijndrecht, Netherlands). The Protein calibration standard II consisting of tripsinongen, Protein A and Bovine serum albumin was purchased from Bruker GmbH (Bremen, Germany) and prepared according to the manufacturer instructions. IgG and IgA were prepared as $2mg.mL^{-1}$ solution in water and then mixed 1:1 (v:v) with a 20 $mg.mL^{-1}$ solution of sinapinic acid prepared in 1:1 acetonitrile:water (v:v) + 0.1% trifluoroacetic acid. Prepared aliquots of Protein Calibration Standard II were mixed 1:1 (v:v) with a 20 $mg.mL^{-1}$ solution of sinapinic acid prepared in 1:1 acetonitrile:water (v:v). 1 µL aliquots of each analyte:matrix solution were then deposited onto a stainless steel target plate and air dried prior to analysis.

Mass Spectrometry

All mass spectrometry experiments were performed on an Ultraflex III MALDI time-of-flight mass spectrometer (Bruker Daltonik GmbH, Bremen, Germany) equipped with a Smartbeam 355 nm Nd:YAG laser and with an ion acceleration voltage of 25 kV. A schematic of the experiential setup is shown in Figure S1 below. All spectra were acquired by summing 500 laser shots, with the exception of the IgA spectra that were acquired by summing 5000 laser shots. The conventional detector assembly was replaced with the Timepix assembly described above. The laser was operated at a frequency of 10 Hz and a laser power of 52% (offset 65%, range 20%, manufacturers units) was used for IgG and protein mix analysis and 62% (offset 65%, range 20%) for IgA experiments. Analysis of the 22-66kDa Protein Calibration Standard II was performed with an extraction voltage of 1.9 kV, lens voltage of 6 kV and a pulsed ion extraction delay of 500 ns. IgG and IgA spectra were both acquired with an extraction voltage of 4 kV, lens voltage of 12 kV and pulsed ion extraction delays of 500 ns and 1000 ns, respectively. For all spectra mass calibration was achieved using calibration coefficients generated by analysis of Protein Calibration Standard II with the same instrument parameters.

Acquisition of spectra with the standard analog-to-digital converter (ADC) was achieved by decoupling the current pulse from the high voltage line of the MCP backside of the home-built MCP-Timepix detector assembly (Figure S1).[3] This signal is the fed into a homemade preamplifier and then fed into the standard ADC card of the UltraflexIII. All MCP spectra were acquired with a digitization rate of 100 MHz. Where mentioned, baseline subtraction was performed using the derivative baseline correction algorithm.[7]

For acquisition of the IgA spectrum in Figure 2, two spectral windows were acquired and then stitched together. The first spectrum was acquired with an acquisition window

beginning 415 µs after the laser shot such that doubly charged IgA is one of the first arriving ions. The second window was acquired with a delay of 600 µs such that single charged IgA is one of the first arriving ions.

Figure S1

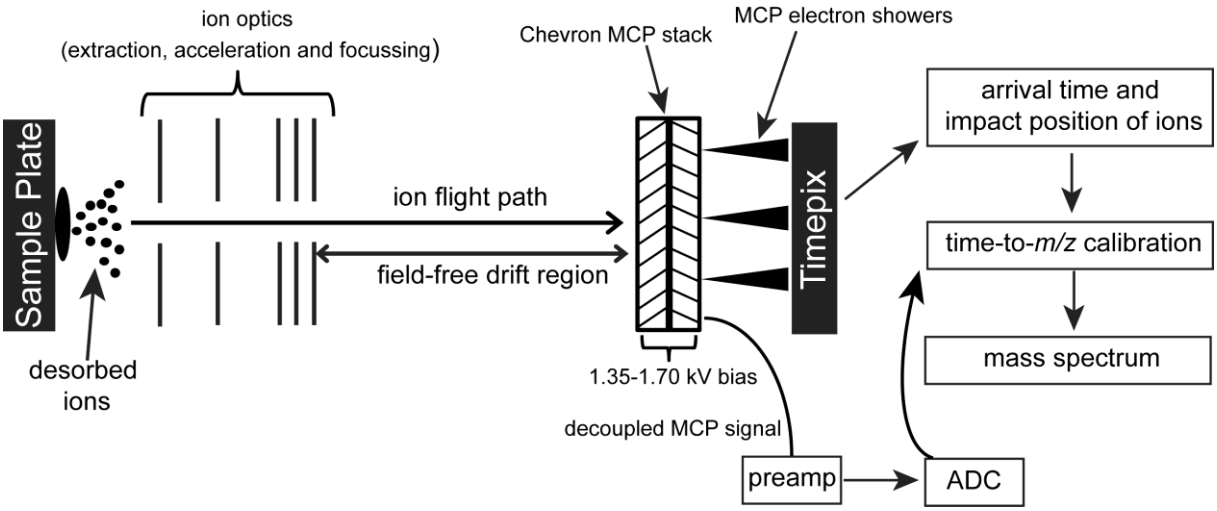

Figure S1. Instrument and acquisition schematic.

Additional Figures

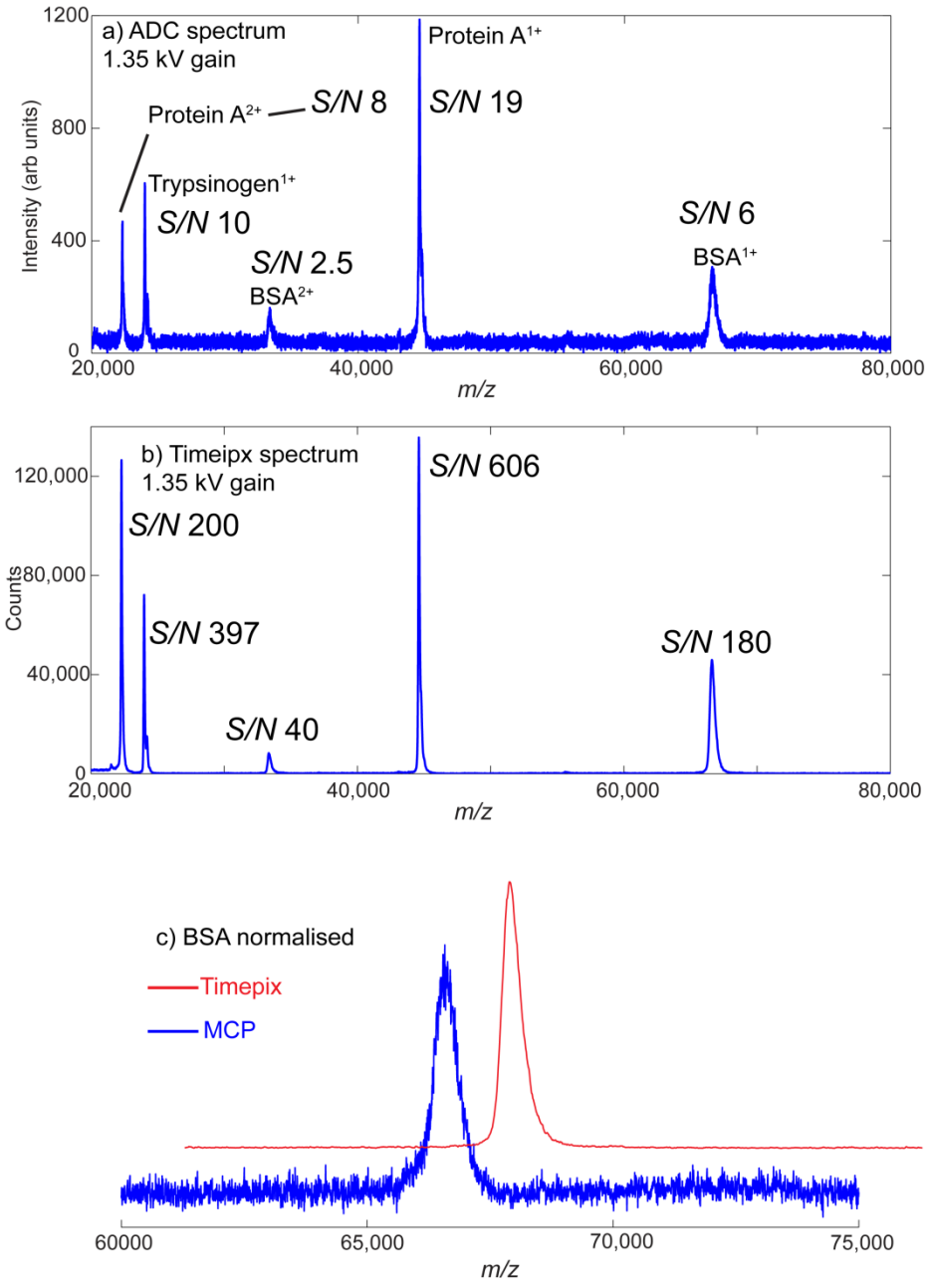

Figure S2. MALDI-TOF-MS mass spectra of a protein mixture consisting of Protein A, trypsinogen and Bovine serum albumin (BSA) acquired using (a) the decoupled MCP signal with an ADC following baseline correction and (b) the Timepix detector without any post-processing Both spectra were acquired in parallel with an MCP bias of 1.35 kV and represent the accumulation of 500 laser shots. (c) Offset overlay of normalised BSA signal recorded with the ADC system (shown in blue) and the Timepix (shown in red) highlighting the significant improvement in signal-to-noise when acquired with the Timepix.

Figure S3

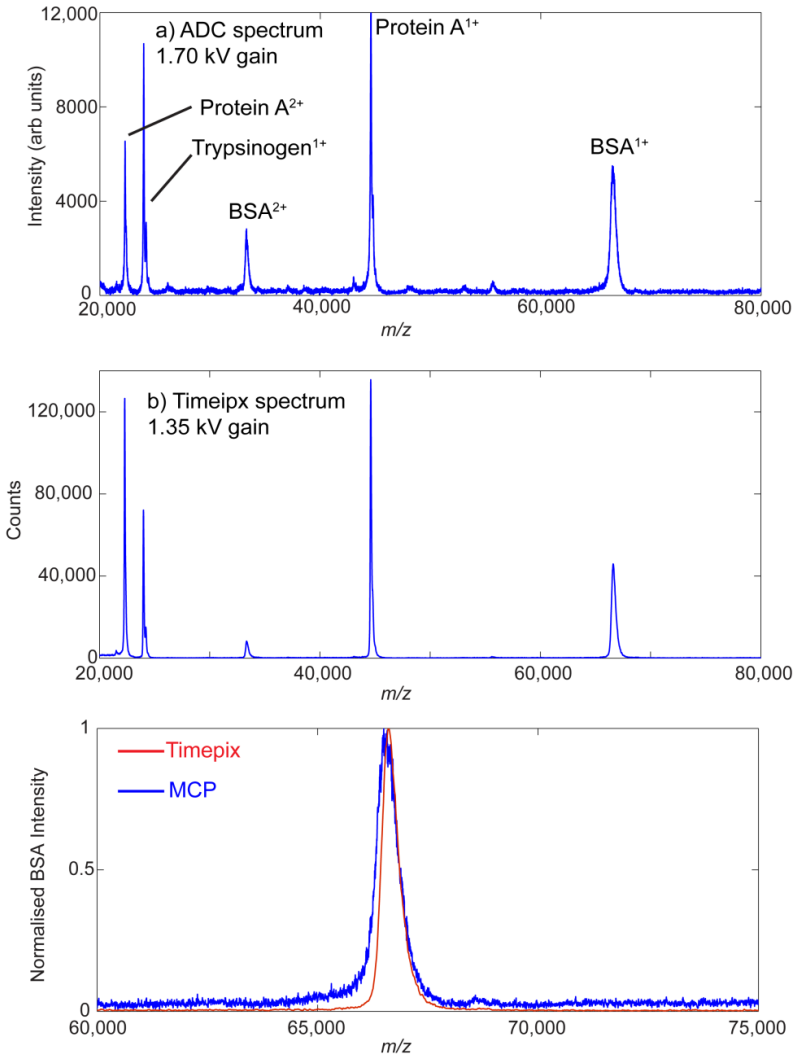

Figure S3. MALDI-TOF-MS spectra of a protein mixture consisting of Protein A, trypsinogen and Bovine serum albumin (BSA) acquired using (a) the decoupled MCP signal with an analog-to-digital converter (ADC) following baseline correction and with an MCP bias of 1.70 kV and (b) the Timepix detector without any post-processing acquired with an MCP bias of 1.35 kV. Both spectra represent the accumulation of 500 laser shots. Overlay of intensity normalised BSA signal recorded in (a) and (b) with the ADC system (shown in blue) and the Timepix (shown in red) highlighting the significant improvement in signal-to-noise when acquired with the Timepix. Note the low abundance peaks between *m/z* 40,000 and 60,000 in the ADC are either observed at low abundance or absent in the Timepix spectrum due to the single-stop TDC of the Timepix and the fact that the highly abundant Protein A^{1+} ion (m/z 44613) is focussed to a similar area of the detector. This effect can thus mask the detection of low abundance, heavier ions. This effect may be minimised by adjusting the ion extraction parameters and running at lower MCP gains.

Figure S4

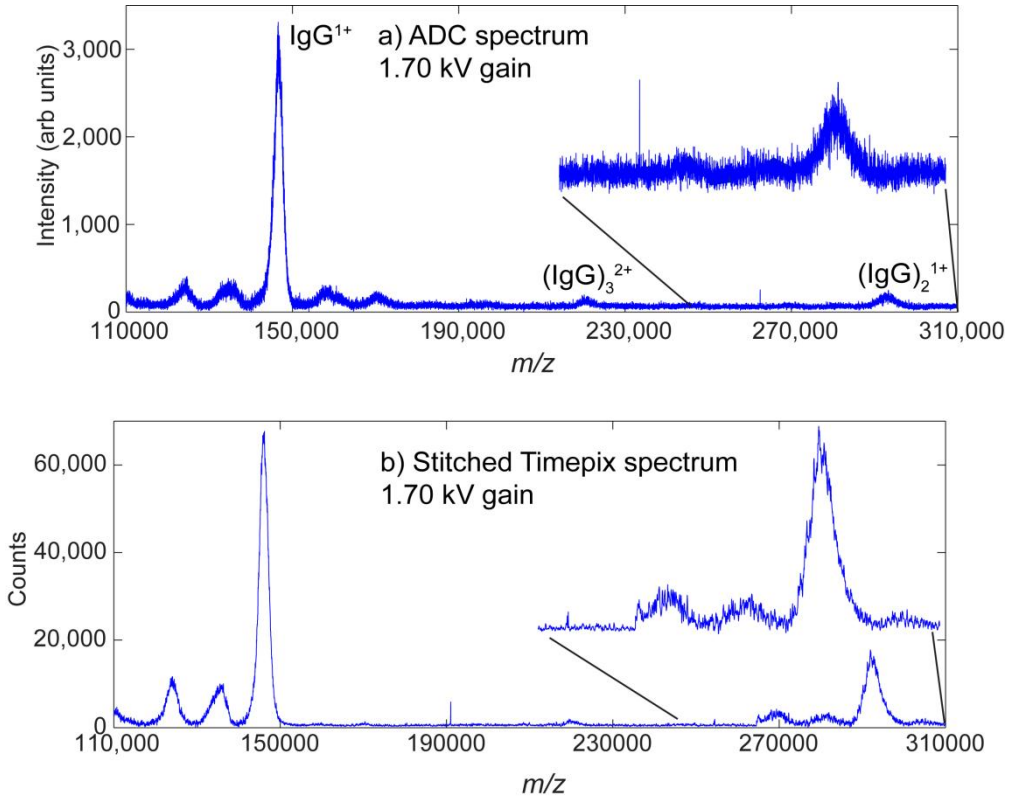

Figure S4. (a) MALDI-TOF spectrum of Immunoglobulin G (IgG) acquired using the decoupled MCP signal in combination with an ADC. (b) Corresponding IgG spectrum acquired with the Timepix system. The insets show the magnified *m/*z 250,000-310,000 region for each spectrum. All spectra were baseline corrected and were acquired from the accumulation of 500 laser shots and an MCP bias of 1.70 kV.

Figure S5

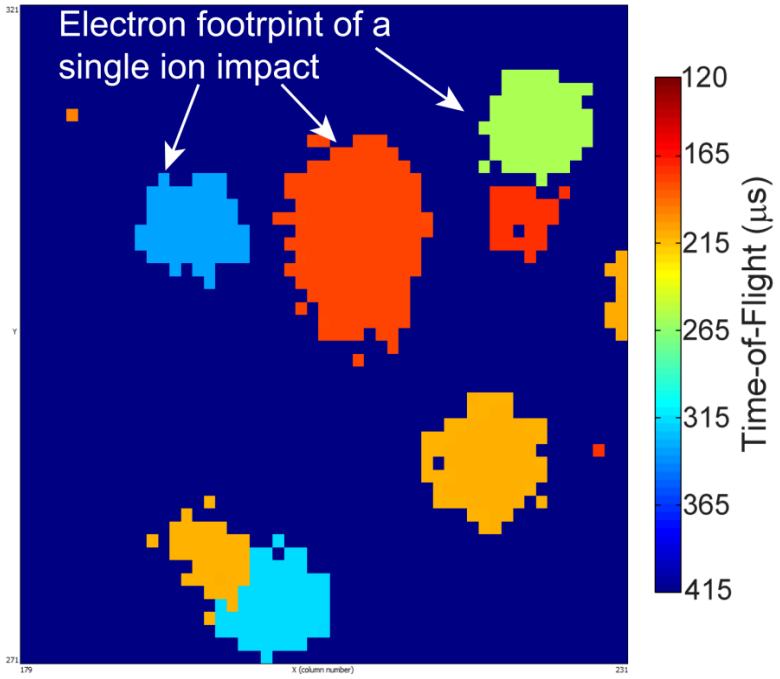

Figure S5. Snapshot of a section for a single Timepix frame (*i.e.*, acquired from a single laser shot). Each ion hit creates an electron shower that activates multiple pixels. Different colours correspond to different arrival times and therefore different *m/z* values.

Figure S6

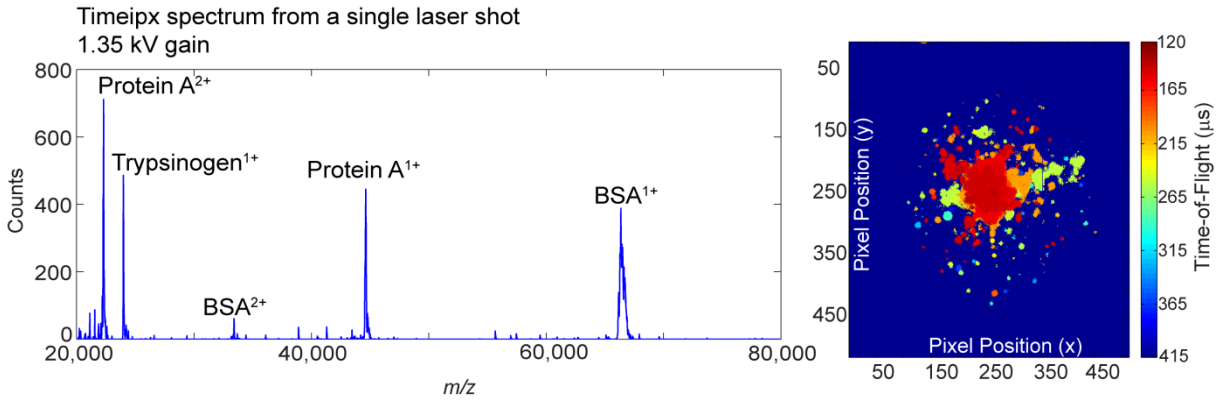

Figure S6. Timepix mass spectrum generated from a single laser shot acquired during acquisition of Figure 1b. The figure on the right shows the corresponding single laser shot Timepix frame that produces the spectrum show on the left.

Figure S7

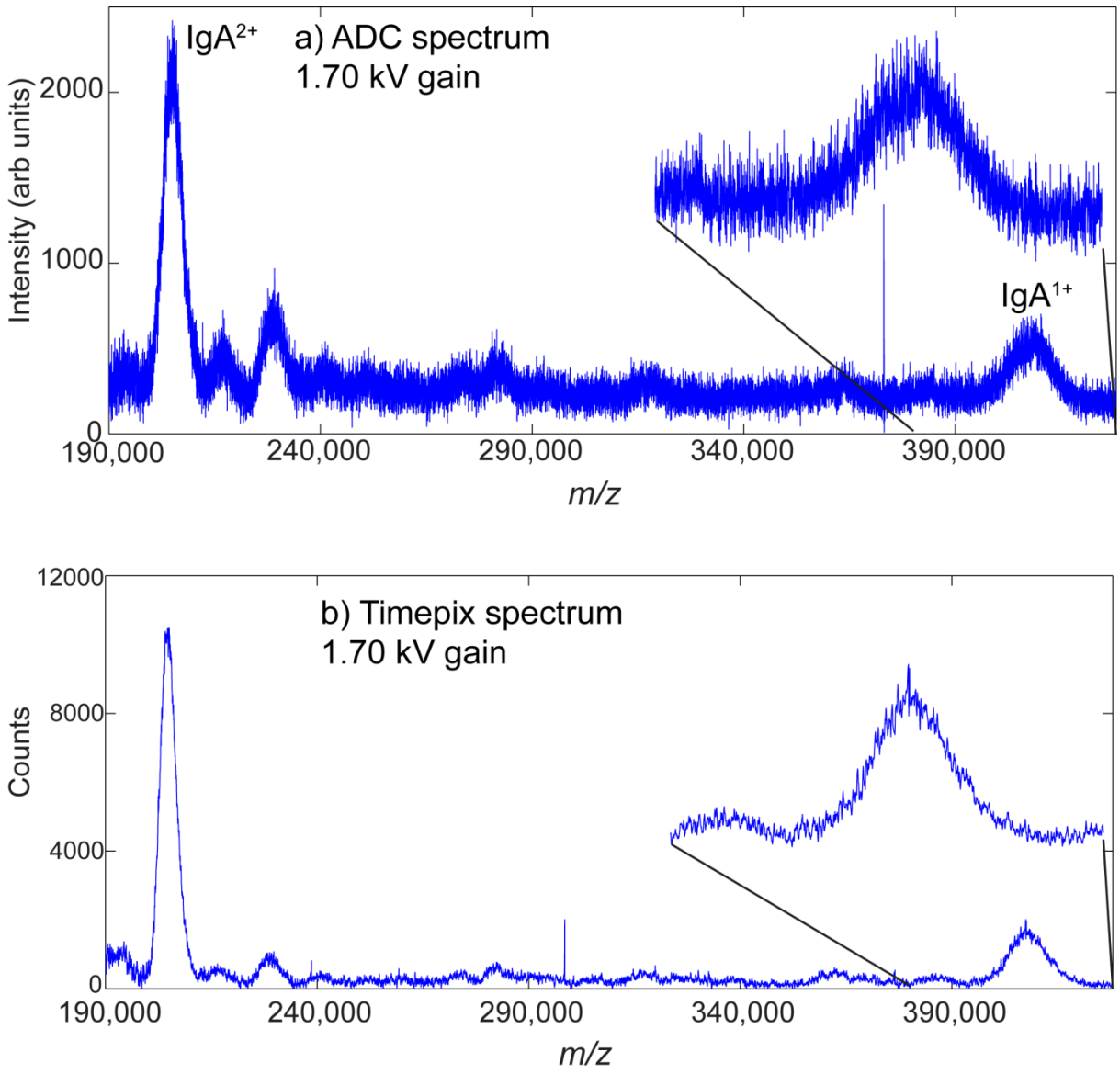

Figure S7. (a) MALDI-TOF mass spectrum of Immunoglobulin A (IgA) acquired using the decoupled MCP signal in combination with an ADC. (b) Corresponding IgG spectrum acquired with the Timepix system acquired during single acquisition window. Both spectra were baseline corrected and were acquired with an MCP bias of 1.70 KV and the accumulation of 5000 laser shots. The insets show the magnified *m/z* 380000-430000 region for each spectrum. Baseline correction was performed for the Timepix spectrum due to the high chemical background present in the spectrum.

References

[1] a) X. Llopart, M. Campbell, R. Dinapoli, D. San Segundo, E. Pernigotti, *IEEE Trans. Nucl. Sci.* **2002**, *49*, 2279; b) X. Llopart, M. Campbell, *Nucl. Instrum. Methods. Phys. Res. A.* **2003**, *509*, 157.

[2] X. Llopart, R. Ballabriga, M. Campbell, L. Tlustos, W. Wong, *Nucl. Instrum. Methods. Phys. Res. A.* **2007**, *581*, 485.

[3] J. H. Jungmann, L. MacAleese, J. Visser, M. J. J. Vrakking, R. M. A. Heeren, *Anal. Chem.* **2011**, *83*, 7888.

[4] A. Kiss, J. H. Jungmann, D. F. Smith, R. M. A. Heeren, *Rev. Sci. Instrum.* **2013**, *84*, 013704.

[5] a) T. Holy, J. Jakubek, S. Pospisil, J. Uher, D. Vavrik, Z. Vykydal, *Nucl. Instrum. Methods. Phys. Res. A.* **2006**, *563*, 254; b) D. Turecek, T. Holy, J. Jakubek, S. Pospisil, Z. Vykydal, *J. Instrum.* **2011**, *6*, C01046.

[6] J. Visser, B. van der Heijden, S. J. A. Weijers, R. de Vries, J. L. Visschers, *Nucl. Instrum. Methods. Phys. Res. A.* **2011**, *633, Supplement 1*, S22.

[7] G. B. Eijkel, B. Kükrer Kaletaş, I. M. van der Wiel, J. M. Kros, T. M. Luider, R. M. A. Heeren, *Surf. Interface Anal.* **2009**, *41*, 675.